Fourier summation, FORDAP; least-squares refinement, OR XLFS3; error analysis of distances and angles, OR FFE3, and structural drawings, OR TEPII. For determination of least-squares planes the program PLNJO was used; J.-O. Lundgren, University of Uppsala, Uppsala, Sweden; based on the method of D. Blow, *Acta Crystallogr.*, **13**, 168 (1960). For the intensity statistics MULTAN was used; J. P. Declercq, G. Germain, P. Main, and M. M. Woolfson, *Acta Crystallogr., Sect. A*, **29**, 231 (1973). The Delauney-reduced cell parameters were derived using the computer program TRACER II, A Fortran Lattice Transformation-Cell Reduction Program, written by Dr. S. L. Lawton.
(17) P. Day and J. Hines, *Operating Systems Rev.*, **7**, 28 (1973).
(18) S. W. Peterson and H. A. Levy, *Acta Crystallogr.*, **10**, 70 (1957).
(19) (a) The Zachariasen approximation[19b] was used for the overall isotropic g parameter as defined and scaled by Coppens and Hamilton.[19c] The $|F_o|$ values were corrected for extinction from the expression $|F_o|_{corr} = |F_o|(1 + \bar{T}2g\lambda^3|F_c|^2/V^2 \sin 2\theta)^{-1/4}$, where $|F_c|$ is on an absolute scale, λ is the wavelength (Å), g is the refined extinction parameter, $\bar{T}$ is the mean absorption-weighted path length in the crystal in centimeters (calculated simultaneously during the computation of absorption corrections), and V is the unit cell volume (Å^3). (b) W. H. Zachariasen, *Acta Crystallogr.*, **23**, 558 (1967). (c) P. Coppens and W. C. Hamilton, *Acta Crystallogr., Sect. A*, **26**, 71 (1970).
(20) G. E. Bacon, *Acta Crystallogr., Sect. A*, **8**, 357 (1972).
(21) M. L. Moreau-Colin, *Bull. Soc. Fr. Mineral. Cristallogr.*, **91**, 332 (1968).
(22) K. Krogmann, *Angew Chem., Int. Ed. Engl.*, **8**, 35 (1969).
(23) Some very short Pt–Pt separations are: (a) 2.58 (1) Å in $[Pt_3(C_8H_{12})_3(SnCl_3)_2]$, L. J. Guggenberger, *Chem. Commun.*, 512 (1968); (b) 2.581 Å in $[Pt_2(\pi\text{-}C_5H_5)_4]$, K. K. Cheung, R. J. Cross, K. P. Forrest, R. Wardle, and M. Mercer, *Chem. Commun.*, 875 (1971); (c) 2.675 (1) Å in $Pt_3[P(C_6H_{11})_3]_4(CO)_3$, A. Albinati, G. Carturan, and A. Musco, *Inorg. Chim. Acta*, **16**, L3-L4 (1976); (d) 2.647 Å in $[Pt_2S(CO)(PPh_3)_3]$, A. C. Skapski and P. G. H. Troughton, *J. Chem. Soc. A*, 2772 (1969); and (e) J. M. Williams, *Inorg. Nucl. Chem. Lett.*, **12**, 651 (1976).
(24) P. L. Johnson, T. R. Koch, J. A. Abys, and J. M. Williams, to be published.
(25) K. Krogmann, *ACS Symp. Ser.*, **5**, (1974).
(26) J. Bernasconi, P. Bruesch, D. Kuse, and H. R. Zeller, *J. Phys. Chem. Solids*, **35**, 145 (1974).
(27) R. L. Musselman, T. R. Koch, and J. M. Williams, to be published.
(28) T. W. Thomas, C.-H. Hsu, M. M. Labes, P. S. Gomm, A. E. Underhill, and D. M. Watkins, *J. Chem. Soc., Dalton Trans.*, 2050 (1972).
(29) K. Carneiro, J. Eckert, G. Shirane, and J. M. Williams, *Solid State Commun.*, in press.
(30) A. J. Schultz, G. D. Stucky, and J. M. Williams, to be published.
(31) R. Comes, M. Lambert, H. Launois, and H. R. Zeller, *Phys. Rev. B*, **8**, 571 (1973); R. Comes, M. Lambert, and H. R. Zeller, *Phys. Status Solidi B*, **58**, 587 (1973).
(32) L. Pauling, "The Nature of the Chemical Bond", 3d ed, Cornell University Press, Ithaca, N.Y., 1960.
(33) J. R. Ferraro, L. J. Basile, and J. M. Williams, *J. Chem. Phys.*, **64**, 732 (1976).
(34) D. Cahen and J. E. Lester, *Chem. Phys. Lett.*, **18**, 108 (1973).
(35) M. A. Butler, D. L. Rousseau, and D. N. E. Buchanan, *Phys. Rev. B*, **7**, 61 (1973).
(36) P. L. Johnson, T. R. Koch, and J. M. Williams, to be published.
(37) C. F. Eagen, S. A. Werner, and R. B. Saillant, *Phys. Rev. B*, **12**, 2036 (1975). Note that the charge density wave distortions in KCP(Br) are small and the rigid sinusoidal displacement of the $Pt(CN)_4^{-2}$ groups (at 7 K) amounts to only 0.026 Å.

Contribution from the Chemistry Division, Argonne National Laboratory, Argonne, Illinois 60439, and the Webster Research Center, Xerox Corporation, Webster, New York 14580

The Nature of the Pt Chain Distortion in the Partially Oxidized One-Dimensional Complex, $K_{1.75}Pt(CN)_4 \cdot 1.5H_2O$[1]

A. H. REIS, Jr., S. W. PETERSON,* D. M. WASHECHECK,[2] and JOEL S. MILLER[3]

Received March 22, 1976 AIC60199Y

The oxidation of potassium tetracyanoplatinate(II) in the absence of halide ions results in the formation of bronze needles of $K_{1.75}Pt(CN)_4 \cdot 1.5H_2O$ stoichiometry. The structure of this partially oxidized material consists of parallel one-dimensional noncollinear chains involving a commensurate repeat unit of 11.865 Å. Thus the unit cell contents as deduced from single crystal x-ray data is formulated $K_7[Pt(CN)_4]_4 \cdot 6H_2O$ and is stoichiometric. This material crystallizes in the triclinic space group $P\bar{1}$ with a = 10.323 (14), b = 9.285 (13), c = 11.865 (17) Å, α = 77.31 (3), β = 114.85 (5), γ = 73.84 (2)°, and Z = 4. The structure was solved by a combination of Patterson, Fourier, and least-squares refinement techniques to an R_F = 0.050 for the 1840 observed reflections for which $F_o > 3\sigma F_o$. There are three inequivalent Pt atoms in the chain and two Pt–Pt bond distances of 2.967 (1) and 2.976 (1) Å. The average twist angles of the cyanide ligands of the tetracyanoplatinate planes are 45.3 (5) and 49.8 (3.7°). An extensive network of K^+ ionic bonding and hydrogen bonded water molecules knit the material together orthogonal to the chain direction. The chain distortion is shown to be due to Coulombic forces acting between the tetracyanoplatinate anions, located in the asymmetric crystal sites at $z = \sim 1/4$ and $3/4$, and the coordinated asymmetric K^+ distribution. The crystallographic analysis leads to the formal oxidation state of +2.25 for Pt in this potassium deficient material and an odd number of electrons per unit cell.

Introduction

In recent years there has been an enhanced interest in the chemical and physical properties of pseudo-one-dimensional inorganic and organic complexes due to the prediction and observation of a number of unusual anisotropic physical phenomena[4-6] (e.g., high conductivity, metallic state, metal insulator transition, charge density wave, superconductivity) and chemical properties (e.g., novel structures containing infinite chains with short interplanar spacings, homogeneous nonstoichiometric compositions, and mixed valency) directly associated with the reduced dimensionality of various one-dimensional systems.[6-8]

For these reasons there has been immense interest in the synthesis and characterization of several partially oxidized one-dimensional materials. The best characterized highly conducting one-dimensional complexes are based on the partial oxidation of tetracyanoplatinate(II) and reduction of 7,7,-8,8-tetracyano-*p*-quinodimethane.[6] Partial oxidation of tetracyanoplatinate(II) in the presence of chloride or bromide results in the formation of $K_2Pt(CN)_4X_{0.3} \cdot 3H_2O$ (X = Cl, Br) which are well characterized at several temperatures by x-ray,[9-10] neutron,[11-14] and diffuse scattering[15] methods and have an incommensurate superlattice which is attributed to a charge density wave instability.[16]

Oxidation of tetracyanoplatinate(II) in the absence of halide ions was shown by Levy in 1910[17] to yield a complex of nominal $K_{1.75}Pt(CN)_4 \cdot 1.5H_2O$[17,18] stoichiometry. This bronze material was initially characterized by short interplanar spacings from x-ray powder analysis[18] and conductivity[19] which increased with decreasing temperature[19a] thereby suggesting a metallic state. With the isolation of single crystals suitable for x-ray[20] and neutron[21] analysis the structural determination of this partially oxidized cation deficient complex of $K_{1.75}Pt(CN)_4 \cdot 1.5H_2O$, KDEF, has been completed. We are presenting here the results of the complete structural investigation which has been undertaken to characterize the nature of this cation deficient partially oxidized material and determine the driving force behind the Pt chain distortion.

Experimental Section

Crystal Preparation. KDEF was prepared by the partial oxidation of $K_2Pt(CN)_4 \cdot 3H_2O$ in acid solution with hydrogen peroxide according

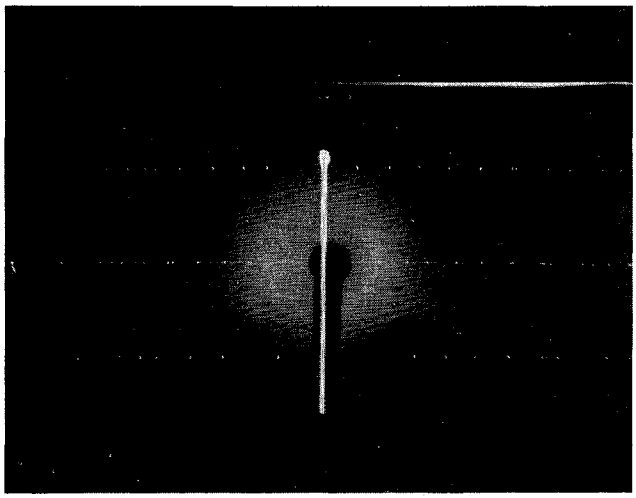

Figure 1. Oscillation photograph of KDEF rotated about the *c* axis showing weak $l \neq 4n$ layers and very strong $l = 4n$ layers with no indication of a superlattice.

to the methods of Levy,[17] Krogmann et al.,[18] and Minot et al.[22] X-ray size crystals grew within 24 h out of the original reaction mixture. Two types of crystals appeared, both metallic needles, a copper form and a bronze form. The copper form was shown to be KCP(Cl), formed due to Cl^- impurities within the original $K_2Pt(CN)_4 \cdot 3H_2O$ starting material. Double aqueous recrystallization of $K_2Pt(CN)_4 \cdot xH_2O$ is adequate to remove chloride impurities. The bronze appearing needles proved to be the desired form of KDEF.

Many of the bronze needle crystals were twinned, the twin axis being the needle axis. A suitable untwinned specimen was selected and mounted in a sealed capillary for preliminary checking and data collection.

Space Group. Preliminary x-ray precession and Weissenberg photographs showed $\bar{1}$ Laue symmetry and no systematic absences consistent with the triclinic space groups $P1$ (C_1, No. 1) or $P\bar{1}$ (C_1^i, No. 2). The crystal needle axis was chosen to be the mounting axis and the crystallographic *c* axis. Oscillation and rotation photographs showed reciprocal lattice layers for which $l = 4n$ were especially strong; all others were very weak (see Figure 1). This result is in contrast to x-ray data for materials such as KCP(Br) and KCP(Cl) where the *c* axis length is about half that of the present case and every $l = 2n$ layer is strong. The strength of the $l = 4n$ and the weakness of $l \neq 4n$ layers clearly indicate the existence of a Pt chain with Pt atoms stacked $\sim c/4$ apart.

X-Ray Data. Table I lists all pertinent experimental information concerned with the data collection and reduction of KDEF. The crystal, sealed in a glass capillary, was mounted on a G.E. XRD-490 automated diffractometer which has been previously discussed in detail.[23] The cell parameters were determined from precise angular measurements of 16 manually centered reflections, chosen in the 2θ range of 20–35°. Two standard reflections were checked repeatedly during the data collection and found to remain unchanged in intensity within the expected statistical variation. Standard errors were assigned to the data on the basis of counting statistics plus a $(0.03I)^2$ contribution to the variance of each reflection.

Structure Solution and Refinement. The structure was solved using a Patterson map which gave large peaks at $c/4$ multiples indicating the positions of the Pt atoms. Space group $P\bar{1}$ was chosen provisionally and Pt(1) and Pt(3) were assigned to the special positions at (0,0,0) and $(0,0,{}^1/_2)$, while Pt(2) was placed at (0.002,0.002,0.252) initially. Isotropic full-matrix least-squares refinement of the scale factor and Pt atoms gave an initial R_F of 0.24. A difference Fourier revealed the positions of the C, N, and K^+ atoms, which were refined isotropically to an R_F of 0.16. The potassium ions and Pt atoms were then refined by anisotropic full-matrix refinement to an R_F of 0.12. A subsequent difference Fourier revealed the positions of all oxygen atoms and a further four cycles of anisotropic full-matrix least-squares refinement converged at an R_F of 0.094. The positions of all hydrogen atoms were found on a final difference Fourier. Anisotropic full-matrix least-squares refinement of all atoms (hydrogens were refined positionally only with a fixed isotropic $B = 4.0$ Å^2) converged to a final R_F of 0.088 for 3067 reflections.

Table I. Experimental Details on $K_{1.75}Pt(CN)_4 \cdot 1.5H_2O$ (KDEF)

Cell constants at $T = 22$ °C: $a = 10.323$ (14) Å, $b = 9.285$ (13) Å, $c = 11.865$ (17) Å, $\alpha = 77.31$ (3)°, $\beta = 114.85$ (5)°, $\gamma = 73.84$ (2)°
Cell volume: 914.25 Å^3
Molecular weight of KDEF: 394.59 g/equiv
Calculated density: 2.866 g cm^{-3}
Measured density: 2.820 (5) by flotation in $CHBr_3/CCl_4$
$Z = 4$
Space group: $P\bar{1}$ [C_1^i, No. 2]
Radiation: Mo Kα, λ 0.710 69 Å (Ross 1, Zr Filter)
Attenuator: Cu foil at 10 000 Hz
Take off angle: 2°
Max 2θ: 50° ($\pm h \pm k + l$)
Scan type: θ–2θ coupled
Scan width: 1.4°
Scan speed: 0.1° step
Counting time: 5 s/step (background 20 s each side of peak)
Crystal:
  c axis mounted
  Volume = 0.3112×10^{-6} cm^3 (0.0060 × 0.0024 × 0.0200 cm)
  Absorption coefficient = 169.80 cm^{-1}
  Max transmission factor = 0.63
  Min transmission factor = 0.40
  No. of reflections collected = 3227
R_F for all reflections = 0.088 (3067)
R_F for reflections where $F_{obsd} > 3\sigma F_{obsd}$ = 0.050 (1840 ref)
$\Sigma_2 = 1.70$

The quantity minimized in the refinement is $\sum w(F_o^2 - F_c^2)^2$ where F_o and F_c are the observed and calculated structure factor amplitudes and the weights *w* are given by $1/\sigma^2(F_o)^2$. The agreement indices are defined as $R_F = \sum ||F_o| - |F_c|| / \sum F_o$, $\Sigma_2 = \sum [w(F_o^2 - F_c^2)^2/(N_O - N_R)]^{1/2}$, where N_O is the number of independent observations and N_R the number of parameters varied. The above R_F values include all the reflections, many of which are unobserved or very weak. The final agreement indices of $R_F = 0.050$ for $F_o > 3\sigma(F_o)$ and $\Sigma_2 = 1.70$ are perhaps more representative in indicating the excellence of the refinement. Since the exact H_2O and K^+ ion composition of the cell was in doubt,[17,18,22] the multipliers of the oxygen atoms and potassium ions were varied in one of the final refinements. The multipliers converged to the following values: K(1), 0.980 (18); K(2), 0.967 (17); K(3), 1.003 (16); K(4), 0.521 (16) (at special position $({}^1/_2,0,0)$); O(1), 1.13 (6); O(2), 0.98 (6); and O(3), 1.00 (6). These results indicate that the K^+ ion and H_2O sites are fully occupied.

The stoichiometry of 3.5 K^+ ions and 3 H_2O molecules in the asymmetric unit was somewhat surprising; although the earliest report[17] had given exactly that stoichiometry, later chemical studies of KDEF[18,22] gave $K_{1.74}Pt(CN)_4 \cdot 1.8H_2O$ and $K_{1.78}[Pt(CN)_4]Br_{0.034} \cdot 2H_2O$ as representing the composition. The equivalence of the materials was verified through comparison of their respective reduced unit cell constants.[20,21] In view of the possibility that halide ion may be incorporated in the lattice a search of the final difference Fourier was made for weak peaks which could be identified with chlorine. Although several weak peaks were found at the noise level of the map (0.3 e$^-$/Å^2) which could be possible halide sites, none were refinable.

The thermal ellipsoid parameters β_{22} (0.0393) for K(4) and β_{11} (0.0263) for O(3) were observed to be relatively large indicating the possibility of disorder and careful examination of the final difference Fourier gave additional credence to this possibility. No other atoms gave any similar indications. Two-position disorder models for both K(4) and O(3) were then incorporated into a least-squares refinement. Both models refined to yield two sites for both K(4) and O(3), however, with no change in the *R* factor. The site separation of the two K^+ sites was 0.72 (2) Å and of the two O sites was 0.76 (6) Å. The anisotropic thermal parameters of N(3) (see Figures 2 and 5a), which is bonded to both K(1) and O(3), show a very small β_{11} (0.0005) contribution and are probably greatly affected by the K(4) and O(3) disorder. Parameter changes for other atoms were insignificant.

Because of the disorder and the space group ambiguity a limited number of attempts were made to refine in the noncentrosymmetric space group $P1$. The large increase in number of parameters prohibited carrying out a complete noncentrosymmetric refinement in $P1$; however, all indications point to $P\bar{1}$ as the correct space group. The existence of disorder in K(4) and O(3) positions, however, if accepted and assumed to be static does imply of course that the local structure

Table II. Fractional Atomic Coordinates for KDEF with Estimated Standard Deviations given in Parentheses

Atoms	x	y	z
Pt(1)	0	0	0
Pt(2)	0.009 26 (10)	−0.021 37 (8)	0.256 65 (9)
Pt(3)	0	0	1/2
C(1)	0.050 (2)	−0.239 (2)	0.054 (2)
N(1)	0.087 (2)	−0.374 (2)	0.085 (2)
C(2)	0.235 (2)	−0.062 (2)	0.097 (2)
N(2)	0.363 (2)	−0.100 (2)	0.148 (2)
C(3)	−0.237 (2)	0.074 (2)	0.402 (2)
N(3)	−0.367 (2)	0.116 (2)	0.349 (2)
C(4)	−0.021 (2)	0.229 (2)	0.446 (2)
N(4)	−0.027 (2)	0.357 (2)	0.412 (2)
C(1)′	−0.119 (2)	−0.152 (2)	0.231 (2)
N(1)′	−0.193 (2)	−0.222 (2)	0.219 (2)
C(2)′	0.134 (2)	0.110 (2)	0.275 (2)
N(2)′	0.205 (2)	0.188 (2)	0.282 (2)
C(3)′	0.198 (2)	−0.236 (2)	0.364 (2)
N(3)′	0.302 (2)	−0.361 (2)	0.428 (2)
C(4)′	−0.185 (2)	0.186 (2)	0.156 (2)
N(4)′	−0.299 (2)	0.303 (2)	0.092 (2)
K(1)	0.400 3 (6)	0.395 5 (5)	0.329 4 (5)
K(2)	−0.269 9 (7)	−0.386 4 (6)	0.392 4 (6)
K(3)	−0.112 5 (5)	0.501 1 (5)	0.129 8 (5)
K(4)	1/2	0	0
O(1)	−0.451 (2)	−0.481 (2)	0.199 (2)
O(2)	−0.446 (2)	−0.170 (2)	0.448 (2)
O(3)	0.365 (2)	0.249 (2)	0.089 (2)
H(1)	0.455 (28)	−0.377 (26)	0.099 (25)
H(2)	−0.482 (27)	0.440 (26)	0.158 (24)
H(3)	0.498 (31)	−0.200 (28)	0.406 (27)
H(4)	−0.408 (29)	−0.104 (27)	0.462 (24)
H(5)	0.470 (30)	0.229 (24)	0.171 (26)
H(6)	0.348 (27)	0.164 (28)	0.136 (24)

is actually noncentrosymmetric and that $P\bar{1}$ applies to the average structure. The atom multipliers were also varied in one of the final refinements of the disordered model. The K^+ ion and H_2O stoichiometry were unchanged.

The atomic coordinates for the average structure of KDEF are listed in Table II and the anisotropic temperature factors are listed in Table III. The Pt, C, N, K^+, and O scattering factors were taken from the compilation of Cromer and Waber[24] and modified for the real and imaginary components of anomalous dispersion.[25] Hydrogen scattering factors were taken from ref 26.

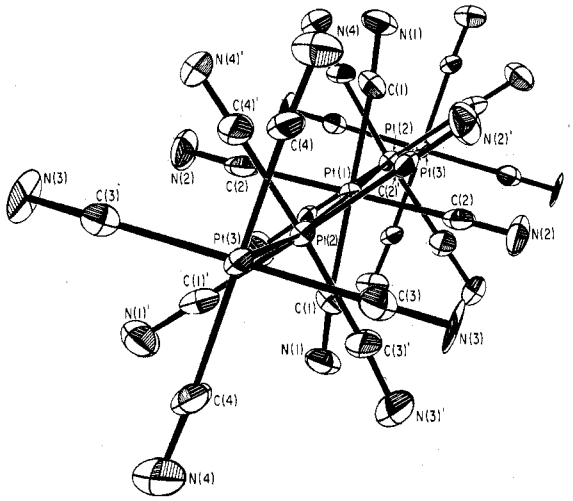

Figure 2. A single wavelength of the Pt atom chain repeat showing atom labeling and staggering of the TCP units along the Pt chain.

The raw x-ray data were reduced using the program DATALIB[27] for input into the Fourier and least-squares refinement programs S5FOUR[28] and S5XFLS,[28] respectively. All distances, angles, and esd's were calculated using the program S5FFE.[28] Molecular drawings were made using the program ORTEP.[29]

Structure Description. The interatomic distances for the structure of KDEF are given in Table IV while the interatomic angles are listed in Table V. Figure 2 depicts positions and labeling for all atoms along the Pt chain.

The crystal structure of KDEF represents a complex mixture of a metal–metal, ionic, and hydrogen-bonded material. An important feature of the structure is the transversely distorted nonlinear Pt atom polymeric chain involving four TCP groups, which lies parallel to the crystallographic *c* axis and shows a repeat of 11.865 (17) Å. Pt(1) and Pt(3) lie at the $\bar{1}$ positions (0,0,0) and (0,0,1/2) while Pt(2) lies at the general position ±(0.009,−0.021,0.256), thus giving rise to a zig-zag chain with the chain sequence ...Pt(2)–Pt(1)–Pt(2)–Pt(3)–Pt(2)–Pt(1).... There are three inequivalent Pt atoms and two unique Pt–Pt distances, Pt(1)–Pt(2) = 2.967 (1) Å and Pt(2)–Pt(3) = 2.976 (1) Å. It is well known that least-squares error estimates for structural parameters are usually underestimated by factors of 2 to 3, thus the

Table III. Anisotropic Thermal Parameters[a] (×10⁴) of KDEF with Estimated Standard Deviations in Parentheses

Atoms	β_{11}	β_{22}	β_{33}	β_{12}	β_{13}	β_{23}
Pt(1)	44.5 (18)	44.8 (13)	48.4 (16)	−16.1 (12)	20.8 (14)	−8.7 (10)
Pt(2)	39.0 (13)	49.4 (10)	45.3 (11)	−11.7 (9)	17.5 (10)	−9.5 (8)
Pt(3)	35.0 (17)	43.6 (13)	44.9 (15)	−7.8 (11)	13.9 (13)	−9.6 (10)
C(1)	86 (29)	83 (27)	115 (19)	−50 (22)	44 (20)	−5 (17)
N(1)	133 (32)	63 (21)	102 (26)	−48 (21)	69 (25)	−18 (18)
C(2)	86 (37)	48 (24)	117 (35)	−29 (23)	10 (30)	7 (22)
N(2)	44 (28)	177 (33)	107 (30)	−35 (24)	20 (24)	−10 (24)
C(3)	98 (39)	63 (25)	119 (34)	−33 (24)	70 (31)	−20 (22)
N(3)	5 (23)	184 (32)	98 (28)	−17 (22)	−5 (21)	−1 (23)
C(4)	51 (25)	51 (23)	120 (20)	−10 (18)	14 (19)	2 (16)
N(4)	143 (33)	76 (22)	74 (23)	−39 (21)	60 (24)	−22 (17)
C(1)′	83 (31)	55 (22)	119 (19)	−1 (20)	37 (21)	12 (15)
N(1)′	129 (33)	97 (24)	96 (27)	−72 (23)	71 (25)	−42 (20)
C(2)′	34 (23)	58 (22)	50 (23)	−1 (19)	17 (20)	6 (17)
N(2)′	101 (30)	150 (29)	73 (25)	−90 (24)	30 (23)	−47 (21)
C(3)′	90 (33)	41 (24)	98 (30)	−24 (23)	42 (27)	−27 (20)
N(3)′	85 (28)	85 (25)	101 (27)	−16 (22)	35 (23)	−21 (20)
C(4)′	84 (32)	73 (26)	87 (29)	−35 (24)	39 (26)	−35 (21)
N(4)′	57 (25)	92 (24)	128 (30)	−11 (21)	42 (24)	−14 (21)
K(1)	93 (8)	141 (8)	100 (8)	−16 (6)	52 (6)	−40 (6)
K(2)	194 (12)	150 (9)	144 (10)	−88 (8)	124 (9)	−66 (7)
K(3)	108 (8)	103 (7)	96 (7)	−50 (5)	54 (6)	−33 (5)
K(4)	97 (14)	393 (27)	166 (17)	36 (14)	75 (13)	115 (15)
O(1)	162 (34)	195 (34)	123 (30)	−27 (24)	40 (26)	−46 (22)
O(2)	105 (30)	175 (32)	104 (27)	−92 (23)	28 (23)	−66 (22)
O(3)	263 (54)	167 (35)	141 (36)	−106 (34)	−91 (33)	44 (26)

[a] The form of the anisotropic temperature factor is: $\exp[-(h^2\beta_{11} + k^2\beta_{22} + l^2\beta_{33} + 2hk\beta_{12} + 2hl\beta_{13} + 2kl\beta_{33})]$.

Table IV. Interatomic Distances for KDEF with Estimated Standard Deviations Given in Parentheses

Atoms	Bond distance, Å	Atoms	Bond distance, Å
(A) Distances within the Pt–Pt Chain			
Pt(1)–Pt(2)	2.967 (1)	Pt(2)–Pt(3)	2.976 (1)
(B) Distances within the TCP(1) Unit which Are Unique (Pt(1) Lies at a Center of Symmetry)			
Pt(1)–C(1)	2.01 (2)	Pt(1)–C(2)	2.03 (2)
C(1)–N(1)	1.13 (2)	C(2)–N(2)	1.10 (3)
(C) Distances within the TCP(2) Unit			
Pt(2)–C(1)′	2.01 (2)	Pt(2)–C(2)′	2.00 (2)
Pt(2)–C(3)′	2.01 (2)	Pt(2)–C(4)′	1.99 (2)
C(1)′–N(1)′	1.12 (2)	C(2)′–N(2)′	1.15 (2)
C(3)′–N(3)′	1.14 (2)	C(4)′–N(4)′	1.15 (2)
(D) Distances within the TCP(3) Unit which Are Unique (Pt(3) Lies at a Center of Symmetry)			
Pt(3)–C(3)	2.03 (2)	Pt(3)–C(4)	2.00 (2)
C(3)–N(3)	1.11 (3)	C(4)–N(4)	1.14 (2)
(E) Distances from the $K^+(1)$ Ion			
K(1)- - -O(2)	2.75 (2)	K(1)- - -N(3)′	2.89 (2)
K(1)- - -O(1)	2.87 (2)	K(1)- - -N(1)	3.00 (2)
K(1)- - -N(3)	2.89 (2)	K(1)- - -N(3)′	3.08 (2)
		K(1)- - -N(2)′	3.13 (2)
(F) Distances from the $K^+(2)$ Ion			
K(2)- - -O(2)	2.70 (2)	K(2)- - -N(3)′	2.99 (2)
K(2)- - -O(1)	2.77 (2)	K(2)- - -N(4)	3.10 (2)
K(2)- - -N(1)′	2.80 (2)		
K(2)- - -N(4)	2.82 (2)		
(G) Distances from the $K^+(3)$ Ion			
K(3)- - -O(3)	2.69 (2)	K(3)- - -N(1)′	3.03 (2)
K(3)- - -N(1)	2.80 (2)	K(3)- - -N(1)	3.11 (2)
K(3)- - -N(4)	2.94 (2)	K(3)- - -N(2)′	3.14 (2)
K(3)- - -N(4)′	2.98 (2)		
(H) Distances from the $K^+(4)$ Ion which Are Unique (Ion Lies on a Center of Symmetry			
K(4)- - -N(2)	2.83 (2)	K(4)- - -O(3)	2.99 (3)
K(4)- - -N(1)′	2.85 (2)		
(I) Distances from O(1)			
O(1)–H(1)	1.13 (24)	O(1)–H(2)	1.01 (23)
O(1)- - -K(2)	2.77 (2)	O(1)- - -K(1)	2.87 (2)
O(1)–H(1)- - -N(4)′	3.00 (3)	O(1)–H(2)- - -N(4)′	3.03 (3)
(J) Distances from O(2)			
O(2)–H(3)	0.75 (26)	O(2)–H(4)	0.81 (25)
O(2)- - -K(2)	2.70 (2)	O(2)- - -K(1)	2.75 (2)
O(2)–H(4)- - -N(2)′	3.05 (2)	O(2)–H(3)- - -N(2)	3.06 (3)
O(2)–H(4)- - -N(3)	3.12 (3)		
(K) Distances from O(3)			
O(3)–H(6)	0.95 (24)	O(3)–H(5)	1.04 (26)
O(3)- - -K(3)	2.69 (2)	O(3)- - -K(4)	2.99 (3)
O(3)–H(5)- - -N(3)	2.82 (3)	O(3)–H(6)- - -N(2)	3.17 (3)
(L) Distances from N(1)			
N(1)- - -K(3)	2.80 (2)	N(1)- - -K(1)	3.00 (2)
N(1)- - -K(3)	3.11 (2)		
(M) Distances from N(2)			
N(2)- - -H(6)	2.39 (23)	N(2)- - -H(6)–O(3)	3.17 (3)
N(2)- - -H(3)	2.59 (27)	N(2)- - -H(3)–O(2)	3.06 (3)
N(2)- - -K(4)	2.83 (2)		
(N) Distances from N(3)			
N(3)- - -H(5)	1.85 (26)	N(3)- - -H(5)–O(3)	2.82 (30)
N(3)- - -H(4)	2.43 (24)	N(3)- - -H(4)–O(2)	3.12 (3)
N(3)- - -K(1)	2.89 (2)		
(O) Distances from N(4)			
N(4)- - -K(2)	2.82 (2)	N(4)- - -K(3)	2.94 (2)
N(4)- - -K(2)	3.10 (2)		
(P) Distances from N(1)′			
N(1)′- - -K(2)	2.80 (2)	N(1)′- - -K(4)	2.85 (2)
N(1)′- - -K(3)	3.03 (2)		
(Q) Distances from N(2)′			
N(2)′- - -K(1)	3.13 (2)	N(2)′- - -H(4)	2.62 (25)[a]
N(2)′- - -K(3)	3.14 (2)	N(2)′- - -H(4)–O(2)	3.05 (3)[a]
(R) Distances from N(3)′			
N(3)′- - -K(1)	2.89 (2)	N(3)′- - -K(2)	2.99 (2)
N(3)′- - -K(1)	3.08 (2)		
(S) Distances from N(4)′			
N(4)′- - -H(1)	1.96 (24)	N(4)′- - -H(1)–O(1)	3.00 (3)
N(4)′- - -H(2)	2.48 (24)	N(4)′- - -H(2)–O(1)	3.03 (3)
N(4)′- - -K(3)	2.98 (2)		

[a] This O–H- - -N interaction although short enough to be considered significant is dubious in view of the poor bonding angle and longer H–N separation. More accurate proton locations may indicate this to be a bifurcated hydrogen bond.

two Pt–Pt separations are not necessarily significantly different. The Pt–Pt distances are on the order of 0.1 Å longer than those found in KCP(Br) and KCP(Cl) and they appear to correlate with the smaller oxidation state of Pt in KDEF, as depicted in Figure 3. The chain distortion is defined by the displacement of Pt(2) from the chain axes c by 0.198 (1) Å which could also be considered the amplitude of a transverse distortion wave; the Pt(1)–Pt(2)–Pt(3) angle is 173.21 (2)°.

Each Pt atom is bonded to four CN^- ligands extending perpendicular to the Pt chain in an approximate square-planar configuration. These tetracyanoplatinate (TCP) units stack parallel to c, thus resulting in a structure consisting of parallel arrays of TCP units linked by H_2O molecules and K^+ ions. Distances and angles within each TCP unit are given in Tables IV and V, respectively. The average bond distances and angles within each TCP unit are as follows: TCP(1), Pt–C = 2.02 (2) Å, C–N = 1.12 (2) Å, Pt–C–N = 176.6 (21)°; TCP(2), Pt–C = 2.00 (2) Å, C–N = 1.14 (2) Å, Pt–C–N = 177.1 (20)°; TCP(3), Pt–C = 2.02 (2) Å, C–N = 1.12(2) Å, Pt–C–N = 177.4 (21)°. Each TCP unit is staggered with respect to the unit directly above and below it in the chain and nearly but not exactly eclipsed by alternate units. (See Table VI for the various C–Pt–Pt–C dihedral angles along the Pt chain.) The average dihedral angles as shown in Figure 6 are: TCP(1)–TCP(2) = 45.3 (5)°, TCP(1)–TCP(3) = 5.1 (2.1)°, TCP(2)–TCP(3) = 49.8 (3.7)°, and TCP(2)–TCP(2)′ = 1.7 (1.1)°. Each TCP unit is planar with only small deviations from planarity.

The structure contains four types of potassium ions, three in general positions and one in the special position at ($^1/_2$,0,0) or disordered about that position. As can be seen in Figure 4 the K^+ ions line up in rather distinct layers within the KDEF lattice. The coordination spheres

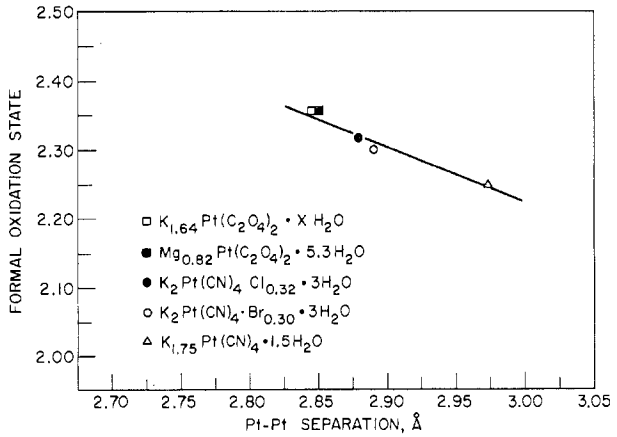

Figure 3. Correlation of the Pt–Pt spacing in various highly conducting inorganic one-dimensional materials with oxidation state.

to 3.3 Å and the associated bond distances for each K^+ ion are shown in Figures 5a–d, while distances and angles are tabulated in Tables IV and V. K(1) and K(3) are both seven-coordinated ions, while K(2) and K(4) show six coordination.

All H_2O molecule hydrogen atoms participate in rather weak hydrogen bonding of the type O–H---N as deduced from the O--N separations which range from 2.82 to 3.17 Å. Each proton is bonded

Table V. Interatomic Angles for KDEF with Estimated Standard Deviations Given in Parentheses

Atoms	Angle, deg	Atoms	Angle, deg
(A) Angles within the Pt-Pt Chain			
Pt(1)-Pt(2)-Pt(3)	173.21 (2)		
(B) Angles within the TCP(1) Unit which Are Unique (Pt(1) at $\bar{1}$)			
Pt(1)-C(1)-N(1)	175.9 (19)	Pt(1)-C(2)-N(2)	177.3 (23)
C(1)-Pt(1)-C(1)	180.0 (0)	C(1)-Pt(1)-C(2)	87.9 (7)
C(2)-Pt(1)-C(2)	180.0 (0)	C(2)-Pt(1)-C(1)	92.1 (7)
(C) Angles within the TCP(2) Unit			
Pt(2)-C(1)'-N(1)'	177.1 (23)	Pt(2)-C(2)'-N(2)'	178.5 (18)
Pt(2)-C(3)'-N(3)'	176.4 (20)	Pt(2)-C(4)'-N(4)'	176.3 (21)
C(1)'-Pt(2)-C(2)'	177.8 (9)	C(3)'-Pt(2)-C(4)'	176.2 (9)
C(1)'-Pt(2)-C(4)'	91.0 (7)	C(1)'-Pt(2)-C(3)'	86.2 (7)
C(2)'-Pt(2)-C(4)'	88.4 (7)	C(2)'-Pt(2)-C(3)'	94.5 (7)
(D) Angles within the TCP(3) Unit which Are Unique (Pt(3) at $\bar{1}$)			
Pt(3)-C(3)-N(3)	179.4 (22)	Pt(3)-C(4)-N(4)	175.5 (21)
C(3)-Pt(3)-C(3)	180.0 (0)	C(3)-Pt(3)-C(4)	87.8 (7)
C(4)-Pt(3)-C(4)	180.0 (0)	C(4)-Pt(3)-C(3)	92.1 (7)
(E) Angles around the $K^+(1)$ Ion			
O(2)-K(1)-O(1)	145.7 (5)	N(3)-K(1)-N(3)'	152.4 (5)
O(2)-K(1)-N(3)	81.9 (5)	N(3)-K(1)-N(1)	127.0 (5)
O(2)-K(1)-N(3)'	86.8 (5)	N(3)-K(1)-N(3)'	79.7 (5)
O(2)-K(1)-N(1)	125.2 (5)	N(3)-K(1)-N(2)'	82.5 (5)
O(2)-K(1)-N(3)'	73.6 (5)	N(3)'-K(1)-N(1)	82.5 (5)
O(2)-K(1)-N(2)'	62.0 (5)	N(3)'-K(1)-N(3)'	79.7 (5)
O(1)-K(1)-N(3)	73.6 (5)	N(3)'-K(1)-N(2)'	114.0 (5)
O(1)-K(1)-N(3)'	104.0 (5)	N(1)-K(1)-N(3)'	146.0 (4)
O(1)-K(1)-N(1)	88.9 (5)	N(1)-K(1)-N(2)'	75.7 (4)
O(1)-K(1)-N(3)'	78.7 (5)	N(3')-K(1)-N(2')	133.9 (5)
O(1)-K(1)-N(2)'	135.0 (6)		
(F) Angles around the $K^+(2)$ Ion			
O(2)-K(2)-O(1)	112.3 (5)	N(1)'-K(2)-N(4)	77.9 (5)
O(2)-K(2)-N(1)'	109.4 (5)	N(1)'-K(2)-N(3)'	164.8 (5)
O(2)-K(2)-N(4)	163.9 (6)	N(1)'-K(2)-N(4)	76.8 (5)
O(2)-K(2)-N(3)'	85.7 (5)	N(4)-K(2)-N(3)'	87.4 (5)
O(2)-K(2)-N(4)	89.4 (5)	N(4)-K(2)-N(4)	78.2 (5)
O(1)-K(2)-N(1)'	92.3 (5)	N(3)'-K(2)-N(4)	103.8 (5)
O(1)-K(2)-N(4)	80.8 (5)		
O(1)-K(2)-N(3)'	81.6 (5)		
O(1)-K(2)-N(4)	158.0 (5)		
(G) Angles around the $K^+(3)$ Ion			
O(3)-K(3)-N(1)	90.5 (7)	N(4)-K(3)-N(4)'	82.3 (5)
O(3)-K(3)-N(4)	133.7 (8)	N(4)-K(3)-N(1)'	72.6 (5)
O(3)-K(3)-N(4)'	88.3 (6)	N(4)-K(3)-N(1)	136.5 (4)
O(3)-K(3)-N(1)'	73.6 (6)	N(4)-K(3)-N(2)'	71.3 (5)
O(3)-K(3)-N(1)	82.5 (7)	N(4)'-K(3)-N(1)'	120.1 (5)
O(3)-K(3)-N(2)'	154.6 (8)	N(4)'-K(3)-N(1)	74.7 (5)
N(1)-K(3)-N(4)	116.6 (5)	N(4)'-K(3)-N(2)'	91.6 (4)
N(1)-K(3)-N(4)'	153.4 (5)	N(1)'-K(3)-N(1)	150.8 (5)
N(1)-K(3)-N(1)'	84.8 (5)	N(1)-K(3)-N(2)'	127.1 (5)
N(1)-K(3)-N(1)	78.7 (5)	N(1)-K(3)-N(2)'	72.9 (5)
N(1)-K(3)-N(2)'	78.4 (5)		
(H) Angles around the $K^+(4)$ Ion			
N(2)-K(4)-N(1)'	90.8 (5)	N(2)-K(4)-N(2)	180.0
N(2)-K(4)-O(3)	65.9 (6)	N(1)'-K(4)-N(1)'	180.0
N(1)'-K(4)-O(3)	107.9 (5)	O(3)-K(4)-O(3)	180.0
N(2)-K(4)-N(1)'	89.1 (5)		
N(2)-K(4)-O(3)	114.0 (6)		
N(1)'-K(4)-O(3)	72.0 (5)		
(I) Angles around O(1)			
H(1)-O(1)-H(2)	88 (17)	O(1)-H(1)- - -N(4)'	149 (15)
O(1)-H(2)- - -N(4)'	112 (16)		
(J) Angles around O(2)			
H(3)-O(2)-H(4)	156 (25)	O(2)-H(4)- - -N(3)	141 (22)
O(2)-H(3)- - -N(2)	123 (23)	O(2)-H(4)- - -N(2)'	113 (19)
(K) Angles around O(3)			
H(6)-O(3)-N(6)	95 (17)	O(3)-H(5)- - -N(3)	152 (17)
O(3)-H(6)- - -N(2)	131 (15)		

to a single N atom; however, in the case of $H_2O(2)$ hydrogen atom H(4) has a close approach to N(2)' as well as N(3) but with a longer H--N separation and an unfavorable bond angle (113°). Each O is

Table VI. Twist Angles along the Pt-Pt Chain in KDEF with Estimated Standard Deviations Given in Parentheses

Atoms	Angle, deg	Atoms	Angle, deg
TCP(1)-TCP(2)		TCP(2)-TCP(3)	
C(1)-Pt(1)-Pt(2)-C(1)'	45.2 (7)	C(4)'-Pt(2)-Pt(3)-C(4)	53.6 (8)
C(2)-Pt(1)-Pt(2)-C(3)'	47.0 (8)	C(2)'-Pt(2)-Pt(3)-C(3)	45.9 (8)
C(1)-Pt(1)-Pt(2)-C(2)'	44.7 (7)	C(3)'-Pt(2)-Pt(3)-C(4)	46.0 (7)
C(2)-Pt(1)-Pt(2)-C(4)'	44.2 (9)	C(1)'-Pt(2)-Pt(3)-C(3)	53.9 (7)
TCP(1)-TCP(2)		TCP(2)-TCP(2)'	
C(1)-Pt(1)-Pt(3)-C(4)	7.2 (7)	C(2)'-Pt(2)-Pt(2)-C(1)'	0.6 (7)
C(2)-Pt(1)-Pt(3)-C(3)	3.0 (6)	C(3)'-Pt(2)-Pt(2)-C(4)'	2.8 (7)
C(1)-Pt(1)-Pt(3)-C(4)	7.2 (7)	C(1)'-Pt(2)-Pt(2)-C(2)'	0.6 (7)
C(2)-Pt(1)-Pt(3)-C(3)	3.0 (6)	C(4)'-Pt(2)-Pt(2)-C(3)'	2.8 (7)

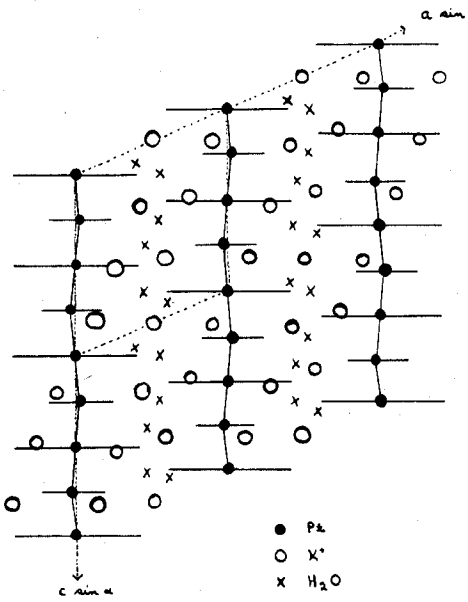

Figure 4. The KDEF lattice projected down the *b* axis showing the Pt atom chains and layers of K^+ ions and H_2O molecules.

tetrahedrally coordinated to two K^+ ions and the two hydrogen atoms. $H_2O(1)$ bridges TCP(2) and TCP(2') units of two parallel Pt chains with O(1)–H(1)---N(4)' = 3.00 (3) Å and O(1)–H(2)---N(4)' = 3.03(3) Å. $H_2O(2)$ and $H_2O(3)$ bridge TCP(1) and TCP(3) units of two parallel Pt chains where O(2)–H(4)---N(3) = 3.12(3) Å, O(2)–H(3)---N(2) = 3.06(3) Å, O(3)–H(5)---N(3) = 2.82(3) Å, and O(3)–H(6)---N(2) = 3.17(3) Å. Thus only N(4)', N(3), and N(2) are involved in hydrogen bonds, each acting as acceptor for two protons. The O–H---N bonds are all nonlinear as is shown by the bond angles given in Table V. The water molecules are distributed roughly in layers parallel to the *c* axis similar to potassium as is shown in Figure 5. The hydrogen bonding and atom packing within the cell are shown by the stereoviews in Figures 6 and 7.

The environment around each N atom in the TCP chain is an indication of the ionic and hydrogen bonding forces acting in concert in the unit cell. Table IV lists close contacts to within 3.3 Å for each N atom. TCP(1) N atoms have the following coordination: N(1)–$3K^+$ ions, N(2)–2H, K^+ ions. Because of the $\bar{1}$ center at Pt(1), the environment of Pt(1) is symmetric. TCP(2) N atoms show the following coordination: N(1)'–$3K^+$ ions, N(2)'–$2K^+$ ions, N(3)'–$3K^+$ ions, and N(4)'–2H, K^+ ion. The environment about Pt(2) is therefore highly asymmetric. The N atoms of TCP(3) show the following coordination: N(3)–2H, K^+ ion and N(4)–$3K^+$ ions. The Pt(3) environment is also symmetric because of the $\bar{1}$ position and is very similar to the Pt(1) environment.

Finally each chain is displaced along *c* with respect to other chains in the cell. This can be seen clearly in Figure 7. This Pt chain displacement or nonalignment is a consequence of the triclinic geometry of the cell and provides better packing of the unit cell constituents.

The K(4) and O(3) disorder previously mentioned is not a major perturbation of the structure; however, the disorder introduces some interesting ramifications. Hexacoordinate K(4) is coordinated by two

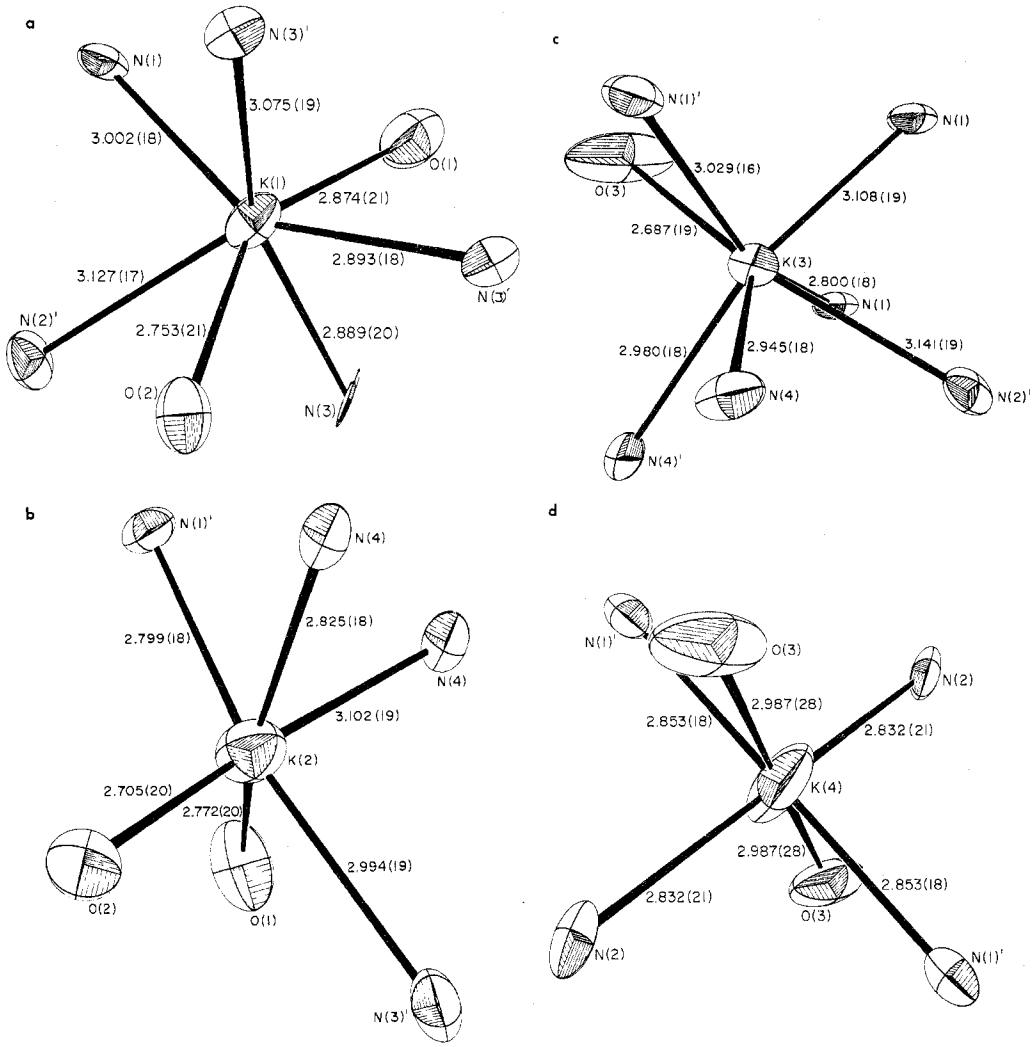

Figure 5. Potassium ion coordination spheres and interaction distances (a) K(1), (b) K(2), (c) K(3), and (d) K(4).

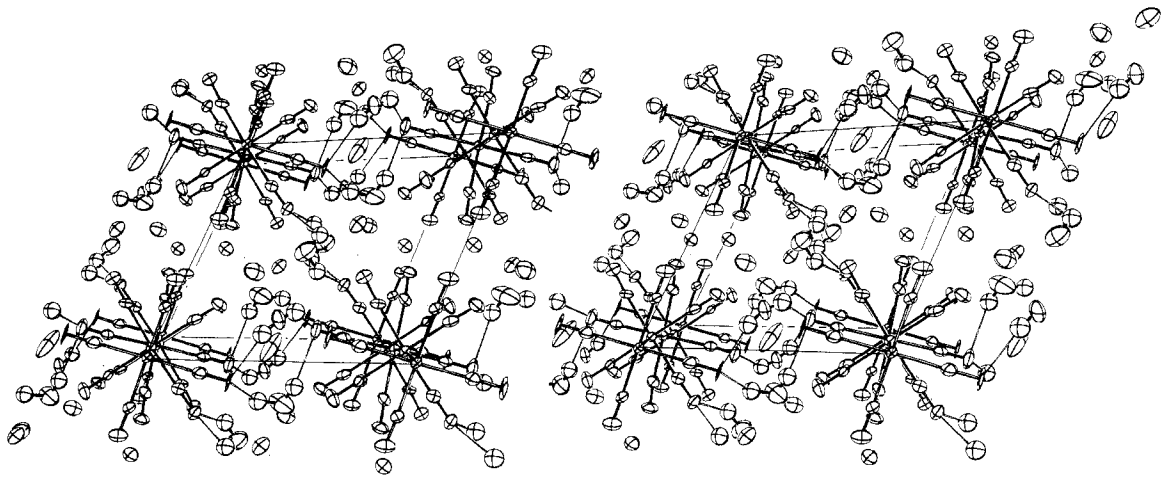

Figure 6. Stereoscopic view of KDEF down the *c* axis showing hydrogen bonding and TCP unit rotation.

O(3) atoms and four N atoms and has two rather long K–O distances of 2.99 Å in the average structure. These are 0.23 Å greater than the average of the remaining K–O distances in this compound. The extension of the K(4) ellipsoid has a large component in the direction of the O(3)–K(4) vector and the disorder sites place K(4) approximately 2.7 and 3.3 Å from the average O(3) position. The result is a shorter K–O distance which is presumably energetically favorable. However, O(3) apparently increases its interactions by simultaneously shifting in its coordination sphere in a direction nearly at right angles to the K(4) shift. If we assume correlated static positions for the disordered K(4) and O(3) we find 2.89 and 2.94 Å as most probable K–O separations. The K(3)–O(3) separations become 2.66 and 2.80 Å as compared to 2.69 Å in the average structure. The K(4) and O(3) interactions with N are not greatly altered. The explanation of the disorder thus appears to lie then in a rather imperfect packing which leaves K(4) with excessive room in which to "rattle" around. $H_2O(3)$ appears to respond to the K(4) shifts in a way which suggests the disorder is dynamic rather than static. The disorder is not necessarily limited to K(4) and O(3); however, the effects must be too small to be observed in the remainder of the structure.

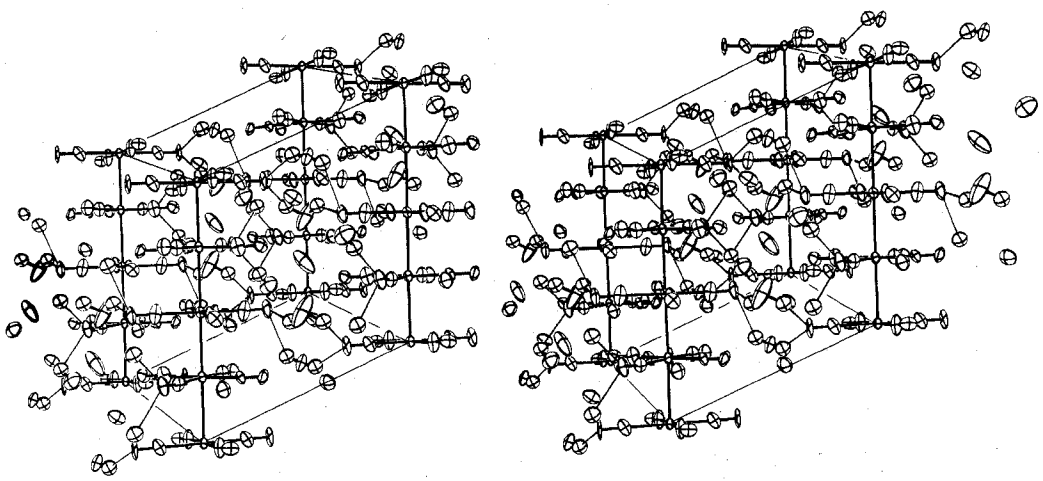

Figure 7. Stereoscopic view of KDEF rotated to show nonalignment of TCP units of several different chains.

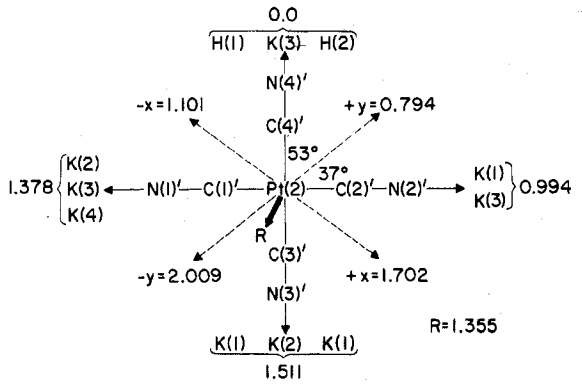

Figure 8. TCP unit 2 showing the resultant K^+ point charges acting on the various CN^- ligands and the resultant Pt chain deformation.

Discussion

The driving force behind the distortion of the TCP chain is of considerable interest, since it might be construed that we are observing the result of a Peierls distortion at room temperature. However, we believe the distortion is not dependent on the electronic structure of the system but is due largely to the electrostatic environment about each TCP unit which we have described above. Our starting point is the idealized undistorted Pt chain with Pt(1) and Pt(3) at (0,0,0) and (0,0,$^1/_2$) and Pt(2) at (0,0,$^1/_4$). Since the environments about Pt(1) and Pt(3) in this model are centrosymmetric, the forces acting upon these Pt atoms are in balance yielding a resultant force of zero. The environment about TCP(2), however, is asymmetric, and we show below that there is a resultant Coulombic restoring force vector which is proportional to the asymmetric charge distribution of K^+ ions and of appropriate magnitude and direction to account for the Pt(2) distortion. Figure 8 shows the TCP(2) unit and the resultant K^+ ion point charges acting on each N atom. The forces which hold the structure together are bonding via band formation, electrostatic, and hydrogen bonding. The assumption is made that the chain distorts because of the unbalanced Coulombic forces on the formally negative charged TCP planes due to the asymmetrically distributed K^+ ions and possibly because of the attractive forces due to hydrogen bonding. On closer examination, the effects of weak hydrogen bonding interactions which operate only on N(4)′ of the Pt(2) cyanoplatinate ion are believed to be negligible since the observed Pt(2) distortion is in a direction nearly opposite to the resultant hydrogen bonding force vector. The attractive force exerted by a K^+ ion coordinated to a Pt(2) cyanide group is to a first approximation given by $q^+q^-/\epsilon r^2$ where q^+ is the point charge on the potassium ion, q^- is the formal −0.4375 point charge on each of the N atoms of the TCP(2), ϵ is the dielectric constant, and r is the separation between the point charges. Since r is roughly the same for all K^+–N interactions and ϵ is assumed to be a constant, the net force on Pt(2) is approximately proportional to the net K^+ ion point charge distribution and may be obtained by summing over all potassium ion–TCP(2) interactions. The sums of the K^+ ion charge components in the direction of the Pt–N vectors are 1.378, 0.994, 1.511, and 0.000 for N(1)′, N(2)′, N(3)′, and N(4)′, respectively. The components along the x and y crystal axes of the resultant charges are then 0.601 and −1.215 which should be proportional to the forces exerted along these directions. These unbalanced point charges acting on the Pt(2) tetracyanoplatinate unit would be expected to displace it until restoring forces set up a new equilibrium. The actual displacement of Pt(2) observed in this study has x and y components of 0.096 and −0.198 Å, respectively. The ratio of magnitudes of the resultant point charges along the x and y axis is −0.495, while the ratio of the Pt(2) shift components in the x and y directions is −0.485.

Clearly the simplified model is in good agreement with the observed direction and relative ratio of the displacement in the x and y directions; however, a more detailed calculation utilizing a charge distribution for the TCP planes, an evaluation of the microscopic dielectric constant, and forces along the chain prohibiting a distortion of the chain is necessary for a quantitative evaluation of the chain distortion. It is also possible to show very approximately that the chief restoring force is the stretching of the Pt(2)–Pt(1) and Pt(2)–Pt(3) bonds. Thus the chain distortion in KDEF appears to be mainly due to the asymmetric K^+ ion distribution.

The Pt–Pt distance in KDEF is ~0.08 Å greater than in KCP(Br) due in part to the lower partial oxidation state (+2.25) compared to the value +2.3 in the latter compound. The higher oxidation state signifies fewer electrons in the conduction band and consequently less Coulombic repulsion, thus shorter interplanar Pt–Pt spacings are anticipated and observed for complexes which have a higher degree of partial oxidation. The two Pt–Pt distances in KDEF differ by 0.009 Å which, if real, may be correlated with the asymmetric K^+ ion distribution. Preliminary conductivity measurements have shown that the conductivity of KDEF is less than that of the other KCP complexes;[19] however, single crystal four probe measurements are necessary to establish the intrinsic electrical properties of this novel system.

The average Pt–C and C–N bond distances are quite similar to previously reported TCP materials. The average Pt–C–N

bond angle is 177.0° thus the configuration is slightly nonlinear as was shown for $K_2Pt(CN)_4 \cdot 3H_2O$[30] and for KCP(Br) and KCP(Cl).[9-14] The strong ligand repulsion is shown by the staggering of the TCP units juxtaposed along the chain. TCP(1) and TCP(3) are not exactly eclipsed perhaps because of the hydrogen bonding water molecules and the unit cell packing.

Conclusions

Although the formula $K_{1.75}Pt(CN)_4 \cdot 1.5H_2O$ appears to be nonstoichiometric, the unit cell is made up of tetrameric units of $K_7[Pt(CN)_4]_4 \cdot 6H_2O$ stoichiometry where the Pt has a formal oxidation state of +2.25. The distorted Pt chain has two crystallographically inequivalent but nearly equal Pt–Pt distances which suggests that the valence electrons on Pt are delocalized over the Pt chain. The Pt chain distortion is due to the asymmetric distribution of attractive forces exerted by the K^+ ions on TCP(2). The H_2O molecules form multiple hydrogen bonds which may contribute to conformation staggering of the TCP(1) and TCP(3) units along the Pt chain. Since the unit cell contains an uneven number of electrons, the possibility of a metallic state is suggested.

Acknowledgment. The authors wish to thank Dr. J. Williams for helpful discussions and for hydrogen atom placement possibilities from neutron Fourier maps and Dr. L. Fuchs for the use of his microscope.

Registry No. $K_{1.75}Pt(CN)_4 \cdot 1.5H_2O$, 59831-03-7.

Supplementary Material Available: Listing of scaled (×0.5) structure factor amplitudes (11 pages). Ordering information is given on any current masthead page.

References and Notes

(1) Work performed under the auspices of the U.S. Energy Research and Development Administration.
(2) Partieipant in the undergraduate research participation program sponsored by the Argonne Center for Educational Affairs.
(3) Xerox Corporation, Webster, N.Y. 14580.
(4) I. F. Shchegolev, *Phys. Status Solidi A*, **12**, 9 (1972).
(5) H. R. Zeller, *Lestkoerperprobleme*, **13**, 31 (1973).
(6) J. S. Miller and A. J. Epstein, *Prog. Inorg. Chem.*, **20**, 1 (1976), and references therein.
(7) K. Krogmann, *Angew. Chem., Int. Ed. Engl.*, **8**, 35 (1969).
(8) T. W. Thomas and A. E. Underhill, *Chem. Soc. Rev.*, **1**, 99 (1972).
(9) H. J. Deiseroth and H. Schulz, *Phys. Rev. Lett.*, **33**, 963 (1974).
(10) H. J. Deiseroth and H. Schulz, *Mater. Res. Bull.*, **10**, 225 (1975).
(11) J. M. Williams, J. L. Petersen, H. M. Gerdes, and S. W. Peterson, *Phys. Rev. Lett.*, **33**, 1079 (1974).
(12) J. M. Williams, M. Iwata, S. W. Peterson, K. A. Leslie, and H. J. Guggenheim, *Phys. Rev. Lett.*, **34**, 1653 (1975).
(13) J. M. Williams, F. K. Ross, M. Iwata, J. L. Petersen, S. W. Peterson, S. C. Lin, and K. Keefer, *Solid State Commun.*, **17**, 45 (1975).
(14) J. M. Williams, M. Iwata, F. K. Ross, J. L. Petersen, and S. W. Peterson, *Mater. Res. Bull.*, **10**, 411 (1975).
(15) R. Comes, *Lect. Notes Phys.*, **34**, 32 (1975); R. Comes, M. Lambert, H. Launois, and H. R. Zeller, *Phys. Rev. B*, **8**, 571 (1973); C. F. Eagen, S. A. Werner, and R. B. Saillant, *ibid.*, **10**, 2036 (1975); B. Renker, H. Rietschel, L. Pintschovius, W. Glaser, P. Bruesel, D. Kuse, and M. J. Rice, *Phys. Rev. Lett.*, **30**, 1144 (1973); B. Renker, L. Pintschovius, W. Glaser, H. Rietschel, R. Comes, and W. Drexel, *ibid.*, **32**, 836 (1974); B. Renker, L. Pintschovius, W. Glaser, H. Rietschel, and R. Comes, *Lect. Notes Phys.*, **34**, 53 (1975).
(16) J. W. Lynn, M. Iizumi, G. Shirane, S. A. Werner, and R. B. Saillant, *Phys. Rev. B*, **10**, 1154 (1975).
(17) L. A. Levy, *J. Chem. Soc.*, 108 (1912).
(18) K. Krogmann and H. D. Hausen, *Z. Naturforsch. B*, **23**, 1111 (1968).
(19) (a) T. W. Thomas, C.-H. Hsu, M. M. Lobes, P. S. Gomm, A. E. Underhill, and D. M. Watkins, *J. Chem. Soc., Dalton Trans.*, 2050 (1972); (b) Y. Hara, I. Shirotani, and A. Onodera, *Solid State Commun.*, **17**, 827 (1975).
(20) A. H. Reis, Jr., S. W. Peterson, D. M. Washecheck, and J. S. Miller, *J. Am. Chem. Soc.*, **98**, 234 (1976).
(21) K. D. Keefer, D. M. Washecheck, N. P. Enright, and J. M. Williams, *J. Am. Chem. Soc.*, **98**, 233 (1976).
(22) M. J. Minot, J. H. Perlstein, and T. J. Kistenmacher, *Solid State Commun.*, **13**, 1319 (1973).
(23) M. E. Druyan, A. H. Reis, Jr., E. Gebert, S. W. Peterson, G. W. Mason, and D. F. Peppard, in press.
(24) "International Tables for X-ray Crystallography", Vol. IV, Kynoch Press, Birmingham, England, 1974, p 71.
(25) Reference 24, p 148.
(26) Reference 24, p 102.
(27) An IBM 370/195 program written by H. A. Levy.
(28) S5FOUR, S5XFLS, and S5FFE are Sigma 5 versions of the programs FOURIER by R. J. Dellaca and W. T. Robinson, ORXFLS3 written by W. R. Busing and H. A. Levy, and ORFFE written by W. R. Busing and H. A. Levy.
(29) "ORTEP" written by C. Johnson, Oak Ridge National Laboratory.
(30) D. M. Washecheck, S. W. Peterson, A. H. Reis, Jr., and J. M. Williams, *Inorg. Chem.*, **15**, 74 (1976).

Contribution from the Departments of Chemistry, Faculty of Engineering Science, Osaka University, Toyonaka, Osaka, Japan 560, and Northwestern University, Evanston, Illinois 60201

Crystal and Molecular Structure of Hydrido(dinitrogen)bis[phenyl(di-*tert*-butyl)phosphine]rhodium(I)

P. R. HOFFMAN,[1a] T. YOSHIDA,[1b] T. OKANO,[1b] S. OTSUKA,[1b] and JAMES A. IBERS*[1a]

Received March 22, 1976 AIC60204Y

The structure of hydrido(dinitrogen)bis[phenyl(di-*tert*-butyl)phosphine]rhodium(I), $RhH(N_2)[P(C_6H_5)(C_4H_9)_2]_2$, has been determined crystallographically. The complex possesses a typical four-coordinate planar geometry about Rh with a slight bending of the phosphine groups toward the hydrido ligand (P–Rh–P = 168.12 (3)°). A linear H–Rh–N–N arrangement is required by the crystallographically imposed twofold axis. The compound crystallizes in space group C_{2h}^6-$C2/c$ of the monoclinic system with four formula units in a cell of dimensions a = 22.187 (2) Å, b = 8.340 (1) Å, c = 15.979 (2) Å, and β = 93.108 (6)°. Important distances are Rh–P = 2.297 (1) Å, Rh–H = 1.66 (5) Å, Rh–N = 1.970 (4) Å, and N–N = 1.074 (7) Å. The structural data were refined by full-matrix least-squares methods to a conventional R index of 0.034 based on those 2760 reflections having $F_o^2 > 3\sigma(F_o^2)$.

Introduction

Dinitrogen complexes of transition metals have held considerable interest since their discovery in 1965.[2] Several of these compounds, most notably those containing Mo or W, have been found to be intriguing starting materials for the conversion of molecular nitrogen to ammonia.[3-8] However, at this time somewhat rigorous conditions must be maintained for the laboratory reduction. Additionally, the nature of the involvement of transition metals in the nitrogen fixation process, i.e., oxidation state, mode of N_2 coordination, etc., still remains unclear.

Structurally dinitrogen has been found to bond to transition metals in three ways: terminally "end-on" (**1**), bridging

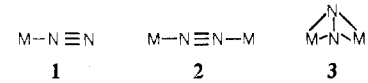

1 **2** **3**

"end-on" (**2**), and bridging "side-on" (**3**).[9,10] The N–N distance in the first two types (1.10–1.12 Å) is only slightly longer than that of free dinitrogen (1.0976 Å) with the exceptions of $ReCl[P(CH_3)_2(C_6H_5)]_4$–$N_2$–$MoCl_4(OCH_3)$[11] and $MoCl_4\{N_2ReCl[P(CH_3)_2(C_6H_5)]_4\}_2$[12] in which the N–N